Published in final edited form as:
Neuroimage. 2009 September ; 47(3): 961–971. doi:10.1016/j.neuroimage.2009.05.025.

Modulation of spontaneous breathing via limbic/paralimbic-bulbar circuitry: An event related fMRI study

Karleyton C. Evans[1], **Darin D. Dougherty**[1], **Annette M. Schmid**[2], **Elizabeth Scannell**[1], **Adrienne McCallister**[1], **Herbert Benson**[3], **Jeffery A. Dusek**[3], and **Sara W. Lazar**[1]

[1]Department of Psychiatry, Massachusetts General Hospital and Harvard Medical School, Boston, MA

[2]Peceptive Informatics, Inc., Waltham, MA

[3]Benson-Henry Institute for Mind Body Medicine, Massachusetts General Hospital, Boston, MA

Abstract

It is well established that pacemaker neurons in the brainstem provide automatic control of breathing for metabolic homeostasis and survival. During waking spontaneous breathing, cognitive and emotional demands can modulate the intrinsic brainstem respiratory rhythm. However the neural circuitry mediating this modulation is unknown. Studies of supra-pontine influences on the control of breathing have implicated limbic/paralimbic-bulbar circuitry, but these studies have been limited to either invasive surgical electrophysiological methods or neuroimaging during substantial respiratory provocation. Here we probed the limbic/paralimbic-bulbar circuitry for respiratory related neural activity during unlabored spontaneous breathing at rest as well as during a challenging cognitive task (sustained random number generation). Functional magnetic resonance imaging (fMRI) with simultaneous physiological monitoring (heart rate, respiratory rate, tidal volume, end-tidal CO_2) was acquired in 14 healthy subjects during each condition. The cognitive task produced expected increases in breathing rate, while end-tidal CO_2 and heart rate did not significantly differ between conditions. The respiratory cycle served as the input function for breath-by-breath, event-related, voxel-wise, random-effects image analyses in SPM5. Main effects analyses (cognitive task + rest) demonstrated the first evidence of coordinated neural activity associated with spontaneous breathing within the medulla, pons, midbrain, amygdala, anterior cingulate and anterior insular cortices. Between-condition paired t-tests (cognitive task > rest) demonstrated modulation within this network localized to the dorsal anterior cingulate and pontine raphe magnus nucleus. We propose that the identified limbic/paralimbic-bulbar circuitry plays a significant role in cognitive and emotional modulation of spontaneous breathing.

Keywords

fMRI; respiration; limbic; brainstem

Introduction

The intrinsic respiratory rhythm in humans is established through an exquisitely precise coordination of pacemaker neurons within the brainstem to meet the continuous metabolic

Correspondence to: Karleyton C. Evans, MD, MSc, Department of Psychiatry, Division of Neurotherapeutics, Massachusetts General Hospital-East, 13th Street, Building 149, Suite 2625, Charlestown, MA 02129, Phone: 617-724-0244, FAX: 617-726-4078, kcevans@partners.org.

requirement for gas exchange (Feldman and Del Negro, 2006). Overt behavioral acts such as speaking and volitional deep breathing originate in the cortex and can over-ride the intrinsic brainstem respiratory rhythm (Loucks et al., 2007; McKay et al., 2003). Also, shifts in cognition and emotional state such as laughter, disgust, stress and panic are known to dramatically influence respiratory rhythm (Boiten, 1998; Masaoka and Homma, 1997; Papp et al., 1997). The respiratory pacemakers in the brainstem have been hypothesized to receive modulating tonic input from higher centers, described as “wakeful drive to breathe” mediated by waking mental activity (Fink, 1961; Hugelin, 1986; Shea, 1996; Shea et al., 1987). The modulation of breathing via emotions and cognitions is thought to originate within limbic/paralimbic circuitry yet the details of these specific respiratory pathways have remained elusive (Guz, 1997; Shea, 1996).

The first evidence for limbic modulation of breathing was provided by the work of Spencer (1896) who examined the effects of cortical stimulation in primates and other mammals. Numerous stimulation studies in animal models followed to implicate modulatory effects on breathing by several limbic/paralimbic regions, notably the amygdala, insula and anterior cingulate cortex (Hugelin, 1986; Mitchell, 1981). In humans, there have been rare studies of direct recording and/or stimulation of limbic/paralimbic regions which have also implicated the amygdala, insula and anterior cingulate cortex as candidate regions involved in the modulation of breathing (Frysinger and Harper, 1989; Halgren et al., 1977; Kaada and Jasper, 1952; Penfield and Faulk, 1955; Pool and Ransohoff, 1949). However, these studies used patient populations and the anesthetic and stimulation techniques employed in many of these early studies may have confounded the interpretation of the limbic/paralimbic findings.

Since the advent of modern neuroimaging, studies employing positron emission tomography (PET) (Colebatch et al., 1991; Ramsay et al., 1993) and functional magnetic resonance imaging (fMRI) (Evans et al., 1999; McKay et al., 2003) during volitional hyperpnea (increased ventilation without change in end-tidal partial pressure of carbon dioxide (PCO_2)) have supported early intra-operative observations of motor-cortical respiratory pathways (Foerster, 1936). Notably, using fMRI, McKay et al. (2003) identified simultaneous activation of the sensory-motor cortex, thalamus, and medulla during hyperpnea. However to date, neuroimaging evidence for limbic/paralimbic involvement in human breathing has been limited to studies of respiratory sensation (e.g., dyspnea, urge to cough) (Banzett et al., 2000; Evans et al., 2002; Liotti et al., 2001; Mazzone et al., 2007; Peiffer et al., 2001; von Leupoldt et al., 2008) and respiratory challenge (e.g., hypercapnia, hypoxia, breath-hold) (Harper et al., 2005; Macefield et al., 2006; Macey et al., 2005). As none of the previous imaging studies examined resting breathing per se, the potential involvement of limbic/paralimbic circuitry in resting spontaneous breathing remains unclear. Moreover, while many investigators have proposed limbic/paralimbic circuitry to underlie the changes in breathing pattern that accompany cognitive tasks and emotional states, the putative elements within this circuitry have yet to be completely delineated (Guz, 1997; Homma and Masaoka, 2008; Shea, 1996).

Significant increases in respiratory frequency (f_R) have been demonstrated as a predominant cardio-respiratory finding during cognitive tasks (Grossman, 1983; Mador and Tobin, 1991; Shea, 1996; Shea et al., 1987). For example Shea and colleagues (Shea et al., 1987) demonstrated significantly increases in f_R in the absence of significant changes in tidal volume (V_T), heart rate and blood pressure during cognitive stimuli (reading) compared to resting conditions. Similar f_R increases have been reported during mental arithmetic,(Mador and Tobin, 1991). Given the specificity for differential f_R responses common to cognitive tasks, we sought to exploit this phenomenon to address hypotheses related to breathing modulation within limbic/paralimbic circuitry. Specifically, there were two central

objectives of the present study. Our first objective was to determine whether in line with the prevailing hypothesis that, limbic/paralimbic circuitry is indeed involved in waking spontaneous breathing in addition to the brainstem respiratory centers. Our second objective was to establish if modulation of neural activity within limbic/paralimbic circuitry corresponded to f_R changes provoked by a demanding cognitive task. Given that the rostral pons has been strongly implicated in modulating f_R respiratory frequency (Lumsden, 1923; St John and Paton, 2004; Younes, 1981), we anticipated coordinated limbic/paralimbic and pontine activity with f_R changes. To achieve these goals we performed event-related fMRI (er-fMRI) analysis on data acquired during waking spontaneous breathing, which promised to confer enhanced sensitivity and temporal resolution over previous imaging studies of respiratory control that used block designs (e.g., Ramsay (1993), McKay (2003)) (Dale, 1999; Mechelli et al., 2003). We focused our er-fMRI investigation on limbic/paralimbic and brainstem circuitry to probe for coordinated neural activity synchronized with the respiratory cycle during unlabored spontaneous breathing. We further examined this circuitry during a demanding cognitive task to identify potential differential neural activity corresponding to changes in breathing frequency induced by an enhanced wakeful drive to breathe.

Experimental Procedures

Subjects

This study was approved and conducted in accordance with guidelines established by the Partners Human Research Committee. Written informed consent was obtained from each subject. The study included 14 healthy individuals (10 male, 4 female), aged 24–49. The subjects were all non-hispanic, white individuals with the exception of 1 African American and 1 Asian subject. All subjects were right-handed and were non-smokers without history of confounding psychiatric, neurological or medical disease as assessed by self-report.

Protocol

Each subject participated in one continuous fMRI time-series comprised of 3 epochs: (1) Baseline (BASE, 6 min), during which subjects were told to relax comfortably; (2) silent random number generation (RNG, 6 min), where subjects were told to engage in the cognitive task of RNG silently, without constrain to the numbers used but without the use of arithmetic or series computations; (3) Meditation (MED, 24 min), subjects were told to “meditate”, although the subjects had no prior formal meditation experience and had been told before entering the scanner to ignore this command. The MED data are not reported here as they were acquired for a separate investigation that compared this cohort of ordinary health individuals with a separate cohort of experienced meditators. To avoid carry-over effects every subject started with the BASE epoch, however the epochs of RNG and MED were counterbalanced across subjects. Importantly, the subjects were intentionally not given any specific instructions in regard to breathing frequency, tidal volume, etc.

Cardio-respiratory Measures and Analysis

Subjects lay supine in the MRI scanner and breathed spontaneously through a simple breathing apparatus attached to the nostrils via Nasal Puffs (Cpap Pro®, Simi Valley, CA), that provided an air-tight seal. Airway flow and PCO_2 were measured via MRI-compatible instruments (MLT300L, ADInstruments, Colorado Springs, CO, and Capstar 100, CWE, Ardmore, PA) connected to the common airway line just distal to the nasal puffs. Heart rate via pulse plethysmograph, as well as airway flow and PCO_2 were digitized and recorded to magnetic disk via an analog to digital recording device (Powerlab ML785/8sp ADInstruments). The onset of each whole brain acquisition was recorded simultaneously

with the physiological signals to facilitate the integrated interpretation of fMRI and respiratory physiological data.

Analysis of physiological data was performed using Chart v5.5 companion software developed for Powerlab (ADInstruments, Colorado Springs, CO). Inspiratory and expiratory onsets were determined from the points at which the airway flow waveform crossed zero liters/min. The variables of inspiratory time (T_I), expiratory time (T_E) and respiratory frequency (f_R) were derived from the airway flow waveform. Tidal volume (V_T) was calculated by integrating the airway flow waveform. Heart rate (beats/min) was computed from the distance between peaks of the pulse plethysmograph waveform. Between-condition paired t-tests were subsequently performed on the condition means calculated for these data.

Neuroimaging Data Acquisition and Analysis

MRI data were obtained using a Sonata 1.5 Tesla whole body high-speed magnetic resonance imaging device equipped for echo planar imaging (EPI) (Siemens Medical Systems, Iselin, NJ) with a 3-axis gradient head coil. Head movement was restricted using foam cushions. After an automated scout image was obtained and shimming procedures performed, two high- resolution 3D MPRAGE sequences (repetition time=7.25 ms, echo time=3 ms, flip angle=7°) with in-plane resolution of 1.3mm and 1mm slice thickness were collected for spatial normalization and positioning of the subsequent scans. Blood oxygenation-level dependent (BOLD) fMRI images were acquired using gradient echo T2*-weighted sequences (repetition time=4 s, echo time=40 ms, flip angle=90°), 25 sagittal slices, with 5mm slice thickness (voxel size 5 × 3.125 × 3.125 mm) and a 1 mm gap between slices.

All image pre-processing and analyses were performed within SPM5 statistical parametric mapping analysis software (Wellcome Department of Cognitive Neurology, London, UK; http://www.fil.ion.ucl.ac.uk/spm). Image pre-processing included: motion correction (realignment and unwarping), co-registration, tissue segmentation, normalization, and smoothing. Specifically, within subjects, all images were realigned to the first image of the fMRI time-series using a least squares approach and a six-parameter (rigid body) voxel-for-voxel transformation. The realignment step included unwarping algorithms that corrected for movement by distortion interactions in regions with prominent air-tissue interface, most susceptible to geometric distortions (e.g., medial temporal lobe and brainstem). Subjects' functional images were then co-registered with their corresponding high-resolution structural MRI images using the 3-dimensional rigid-body model to perform voxel-to-voxel affine transformations. In order to facilitate inter-subject averaging and precision in the identification of the relevant functional anatomy, stereotactic spatial normalization was performed. Normalization involved a twelve-parameter affine transformation and subsequent non-linear deformations as estimated by three dimensional discrete cosine transform basis functions, implemented via a residual least squares method that matched images acquired from the study participants with standardized tissue probability templates (based on Montreal Neurologic Institute (MNI) stereotactic space; http://www.bic.mni.mcgill.ca). Following spatial normalization, scans were smoothed with a 6-mm full-width half-maximum isotropic three-dimensional gaussian filter.

After preprocessing, statistical tests were performed to determine condition related regional BOLD signal changes corresponding to the transitions in the respiratory cycle (e.g., inspiratory onset, expiratory onset). Consistent with other event-related designs, each respiratory transition served as the independent input variable for the SPM fMRI time-series analysis. Two factors related to the inter-event-interval have been identified as crucial to optimizing er-fMRI design efficiency, (1) sufficient inter-event-interval variation or 'jitter' and (2) relatively short inter-event-interval duration (i.e., >1 sec ,<6 sec) (Dale, 1999;

Friston et al., 2007; Miezin et al., 2000). Given sufficient variation observed in spontaneous breathing (Priban, 1963), and typical resting spontaneous respiratory frequencies (e.g., 11–17 breaths/min) (Tobin et al., 1988), we reasoned that er-fMRI design efficiency would be optimized using inspiratory and expiratory transitions as input functions for er-fMRI analyses.

The data were convolved with a hemodynamic response function to model the relationship between neural activity and changes in cerebral blood flow (Friston et al., 2007). The SPM design matrix included the realignment parameters, derived from rigid body motion correction preprocessing transformation (displacements in *x*, *y*, *z* directions as well as roll, pitch, and yaw), as additional regressors of non-interest to model any effects of head movement that persisted after realignment (Friston et al., 1996). Two different sets of analyses were conducted as part of a strategy to account for potential sources of physiological artifact: (1) a primary approach incorporated the global BOLD signal intensity ('global regressor'; calculated for each whole brain volume) into the analytic model as a confounding regressor of non-interest, similar to previous studies (Evans et al., 2002; McKay et al., 2003) and detailed elsewhere (Corfield et al., 2001) and (2) a secondary approach that incorporated the PCO2 ('PCO2 regressor'; interpolated for each whole brain volume) into the analytic model as a confounding regressor of non-interest. Hypotheses as related to the brainstem, limbic, and paralimbic regions (addressed below) were tested as contrasts in which linear compounds of model parameters were evaluated using *t* statistics, which were then transformed to *z*-scores. Specifically, random effects, voxel-wise tests were performed to identify (a) combined main effects of respiratory transition (RNG + BASE; one sample t-test), and (b) between condition effects of respiratory transition (RNG > BASE, RNG < BASE; paired t-tests). For the medulla, the statistical threshold for significance based on region size was $P<12 \times 10^{-3}$ (*Z*-score>3.03). Similarly, for the remaining brainstem regions (pons and midbrain), this threshold was determined to be $P<3.0 \times 10^{-4}$ (*Z*-score>3.34). For the paralimbic/limbic search territory the significance threshold was $P<1.6 \times 10^{-4}$ (*Z*-score>3.60). These thresholds reflect Bonferroni-type corrections for multiple comparisons ($P<0.05$), based on the voxel size (5 × 3.125 × 3.125 mm) and the total volume of the medulla (5.7 cm), upper brainstem (pons and midbrain; 23.8 cm), the paralimbic/limbic search territory (amygdala, hippocampus, insula and anterior cingulate; 43.6 cm) as quantified via established morphometric data (Filipek et al., 1994; Kennedy et al., 1998; Luft et al., 1999; Makris et al., 2006). In addition a cluster threshold ≥ 10 voxels was set to identify loci of potential statistical significance. The size of the limbic/paralimbic search territory could be viewed as relatively large, and vulnerable to Type II error. However the *a priori* components (amygdala, hippocampus, insular and anterior cingulate cortices (ACC; inclusive of rostral, dorsal regions)) were all deemed necessary to comprise the search territory given the preponderance of published findings (reviewed in the Introduction), namely tract-tracing studies, animal and human neurosurgical studies, as well as human neuroimaging studies during respiratory provocation. As a measure to confirm anatomical localization, identified peak clusters were further subjected to region of interest (ROI) analyses performed with the WFU PickAtlas toolbox (an adjunctive component software to SPM5; http://www.fmri.wfubmc.edu/cms/software) (Maldjian et al., 2003), with regional anatomic landmarks and boundaries defined by anatomical automatic labeling (AAL) as described by Tzourio-Mazoyer et al. (2002). As a further confirmatory measure, the SPMs resulting from the voxel-wise analyses were inspected with the aid of co-registered structural MRI data. Regional anatomy was defined using the atlases of Duvernoy (1999), Paxinos and Huang (1995) Mai (1997), as well as Talairach and Tournoux (1988) after transformation of SPM5 MNI coordinates to Talairach stereotactic coordinates (http://imaging.mrc-cbu.cam.ac.uk/imaging/mnitalairach). In order to obviate bias, the entire brain volume for each voxel-wise statistical parametric map was inspected for other activation loci of comparable significance value. However, we only considered such findings as significant

in those cases where the actual probability value met the threshold for family-wise error whole-brain volume correction (FWE, $P<0.05$).

Appreciating that the main effects of condition analyses could be biased by one condition over the other, we also performed secondary fixed effects t-tests of the independent conditions to confirm the primary main effects findings. To further characterize interaction findings (RNG > BASE and RNG < BASE), the peri-event BOLD signal time course was extracted from peak functional clusters localized within hypothesized *a priori* ROIs via the SPM MarsBaR toolbox (http://marsbar.sourceforge.net). Within-subject regional BOLD signal time course for each condition were modeled by calculating an estimate of the BOLD signal at 0 sec, 4 sec, 8 sec, 12 and 16 sec (i.e., 5 TRs including onset) after each inspiratory onset. Group mean peri-event time-course plots were generated for each condition for each functionally defined ROI.

Results

Cardio-respiratory Measurements

The mean cardio-respiratory variables are displayed in Table 1. The respiratory variables for the BASE condition were in the normal resting range, consistent with previously reported values of resting spontaneous ventilation (Bendixen, 1964; West, 1992). Compared to RNG, tidal volume (V_T) was greater during BASE yet this difference did not reach significance. Correspondingly, frequency of respiration (f_R) was greater and inspiratory time (T_I) was shorter during the RNG condition compared to the BASE condition ($P<0.05$). As a result, each subject was essentially isocapnic during the entire fMRI scan; notably intra-individual variance in PCO_2 was less than 1 mmHg on average. Heart rate, PCO_2, and expiratory time (T_E) did not significantly differ between conditions.

Neuroimaging

Results for both the primary (global regressor) and secondary (PCO_2 regressor) analyses were similar. Results for the primary analysis are reported here in the text and associated figures and tables. Results for the secondary analysis are reported in Supplemental Table 1. The combined main effects of condition t-test (RNG + BASE) revealed respiratory cycle-related BOLD signal change in the following *a priori* regions: medulla, rostral pons, midbrain (bilateral red nuclei), right lateral amygdala, bilateral dorsal anterior cingulate cortex (dACC), right anterior insula, and left posterior insula (Table 2, Figures 1–2). The extent of amygdala activity spanned from the lateral amygdaloid nucleus posteriorly to the head of the hippocampus. Regional activity localized to the dACC and left posterior insula was highly significant, surviving not only small volume correction but also whole brain correction. Significant *post-hoc* findings from whole brain (corrected) search included: increased BOLD signal in the left subthalamic nucleus, left putamen, left frontal and temporal regions (Supplemental Table 2).

The between condition paired t-test (RNG > BASE) demonstrated significantly greater BOLD signal in *a priori* regions, including the midline ventral pons and left dACC. The midline pontine activation was localized to the raphe magnus nucleus (RMg) extending dorsally and laterally to the raphe interpositus and gigantocellular reticularis nuclei (Table 2, Figure 3). There was also differentially greater BOLD signal within the right anterior insula, however this locus (x=37, y=6, z=15, Z-score 4.89) failed to meet small volume correction. However, regional activity localized to the dACC survived small volume correction as well as whole brain correction. No other significant loci were identified for the RNG > BASE contrast upon post hoc whole brain (corrected) search. The reverse contrast (RNG < BASE) revealed significantly greater BOLD signal in *a priori* regions, including the right rostral

anterior cingulate cortex (rACC), bilateral amygdalae (sublenticular extended amygdalae; SLEA), dorsal pontomedullary junction (nucleus tractus solitarius (NTS)), rostral pons (reticular nuclei) and midbrain (Table 2, Figure 3). Regional activity localized to the rostral pons survived small volume correction as well as whole brain correction. Significant *post-hoc* findings for the RNG < BASE contrast during whole brain (corrected) search included: the right temporal, right parietal and bilateral occipital regions (Supplemental Table 2).

Regional neural activity within *a priori* regions, demonstrated differential temporal dynamics between conditions, as illustrated in the peri-event time-course plots for *a priori* ROIs (Figure 3). The plots depict modeled peri-event (inspiratory onset) BOLD signal time courses for each condition extracted from functional peak clusters identified by the RNG > BASE and RNG < BASE contrasts. The degree of regional neural synchronization with each breath during a given condition can be inferred by the degree to which the magnitude and temporal dynamics of the associated BOLD signal time course approximates the canonical BOLD fMRI hemodynamic response function (i.e., 4–8 sec peak) (Friston et al., 2007). For the dACC and RMg clusters identified by the RNG > BASE contrast the group average BOLD signal peaked in approximately 4 sec during the RNG condition but failed to meet this profile in the BASE condition, suggesting dACC and RMg regional activity is predominantly synchronized with breath onset during the RNG condition (yellow plots in figure 3.), not the BASE condition (blue plots in figure 3.). In contrast, regional BOLD signal localized to the rACC, SLEA, midbrain, rostral pons and NTS was observed as predominantly synchronized with breath onset during the BASE condition not the RNG condition.

Discussion

Our er-fMRI findings provide the first non-invasive evidence in humans of synchronized neural activity across a distributed limbic/paralimbic-bulbar circuitry during unlabored spontaneous breathing. Main effects of condition analyses (RNG + BASE) identified respiratory related activity in the amygdala, insula and anterior cingulate cortex, as well as the midbrain, pons and medulla. We observed respiratory related modulation within this network during the cognitive task relative to the resting baseline condition (RNG > BASE, RNG < BASE), localized to the amygdala, two functionally distinct divisions of the anterior cingulate cortex, and within the brainstem. In the ensuing discussion we review the regional activity identified in relation to the limited previous knowledge regarding the relationship of spontaneous breathing to the limbic/paralimbic-bulbar circuitry.

Amygdala

In keeping with substantial *a priori* evidence supporting our hypotheses about the amygdala, our main effects finding of robust amygdaloid activity synchronized with every breath in the present er-fMRI study is remarkable. Earlier findings of synchronized amygdaloid activity with the respiratory cycle had only been observed in invasive surgical studies in animals (Kaada, 1951; Zhang et al., 1986), rare single unit recordings in human epilepsy cases (Frysinger and Harper, 1990) and a small sample (N=5) human electroencephalographic study of respiratory-related potentials (Masaoka and Homma, 2000).

Our independent condition t-tests confirmed that respiratory synchronized amygdaloid activity was indeed present during both the BASE and RNG conditions (Supplemental Table 3). The lateral amygdaloid region identified by the main effects of this study is known to share dense reciprocal connections within the brainstem respiratory centers (Gabbott et al., 2005; Onimaru and Homma, 2007; Ricardo and Koh, 1978; Zagon et al., 1994). It is this region and the neighboring central nucleus that have strong projections to the other limbic/paralimbic regions identified by the present study (Buchanan et al., 1994; LeDoux, 2000;

Vertes, 2004). The amygdala is thus well situated to have significant influence on respiration (Homma and Masaoka, 2008). However, we cautiously emphasize that the present study was not designed to discern the directionality (e.g., afferent vs. efferent) of the observed amygdaloid activity. Interestingly however, the possibility of this activity being efferent garners support from recent *in vitro* studies of limbic-bulbar-spinal circuitry in rodents that combined fast-optical imaging with electrophysiological techniques. Onimaru and Homma (2007) demonstrated rhythmic spontaneous burst activity in the piriform/lateral amygdaloid territory that precedes activity within the C4-cervical nerve root (main component of the phrenic nerve, and major efferent to the diaphragm).

In contrast to right lateral amygdala activity observed in the main effects analyses (RNG + BASE), differential (RNG < BASE) respiratory-related amygdaloid activity was seen bilaterally in more dorsal, anterior loci, localized to neurons within the piriform cortex, specifically, the sublenticular extended amygdala (SLEA; Table 2, Figure 3). Several studies of amygdala stimulation in animals support the present findings (Hugelin, 1986; Mitchell, 1981). Importantly, increased phrenic nerve output and ventilation has been reported in cats during stimulation of the ansa lenticularis (a region immediately adjacent to the SLEA) as well as decreased phrenic nerve output and ventilation during stimulation to the lateral and basal amygdaloid nuclei (Bonvallet and Bobo, 1972). Other evidence for amygdaloid influence on respiration is drawn from the work of Masaoka et al. (2003) who reported decreased respiratory rate and loss of respiratory-related potentials in a pre-/post-case series of two epilepsy patients who underwent unilateral lesion to the left amygdaloid region.

Anterior cingulate cortex (ACC)

Similar to the amygdala, regional activity within the ACC was observed to be coordinated with the respiratory cycle. Modulation of this activity occurred within known rostral emotional and dorsal cognitive subdivisions of the ACC (rACC and dACC respectively) (Bush et al., 2000). Akin to the amygdala and other limbic/paralimbic structures identified by the present study, the efferent and afferent connections from the ACC to motor, premotor and brainstem regions make it a suitable candidate to modulate breathing. Specifically the ACC regions identified by the present study (areas 24 and 32) are known to have connections to the central, lateral and basolateral amygdale, as well as the insula, midbrain, and brainstem respiratory centers (Buchanan et al., 1994; Gabbott et al., 2005; Hatanaka et al., 2003; Marchand and Hagino, 1983; Vertes, 2004; Zagon et al., 1994). Single unit recordings in unanesthetized cats have shown small cell populations in ACC area 24 to have coordinated discharge associated with respiration, particularly during waking states. Findings from animal and human studies of electrical stimulation of the ACC have been variable, demonstrating either augmentation or inhibition of respiration (Kaada and Jasper, 1952; Kremer, 1947). However in one study that reported meticulous stimulus parameter optimization (Speakman and Babkin, 1949), distinct functional-anatomical separation of respiratory effects during ACC stimulation was characterized in dogs and cats. Notably, stimulation below the genu (rACC) produced decreased respiratory rate and stimulation above the genu (dACC) produced increased respiratory rate. A similar functional-anatomic categorization may be inferred from the human ACC stimulation study of Pool and Ransohoff (1949). In 12 cases studied, only 4 demonstrated changes in respiration, where increased f_R (up to 13breath/min) was observed in cases of stimulation above the genu and decreased f_R (with one instance of apnea) was observed in cases of stimulation in the immediate vicinity of the genu. The findings from the present study are in accord with the findings from those earlier invasive surgical studies. Notably, increased f_R during the RNG condition was associated with differential BOLD signal localized to the rACC, and resting spontaneous f_R during the BASE condition was associated with differential BOLD signal localized to the dACC (Table 2, Figure 3).

Insula

In addition to the amygdala and ACC, regional activity within the insular cortex was also found to be associated with the respiratory cycle (Table 2, Figure 2). The insula has been referred to as the primary visceral sensorimotor region and is known to have heavy reciprocal connections with both the amygdala and anterior cingulate (Augustine, 1996; Craig, 2002; Mesulam and Mufson, 1982; Mufson and Mesulam, 1982; Shi and Cassell, 1998). Moreover, the insula is known to have strong connections to brainstem centers (Tsumori et al., 2006). Respiratory specific insular connections include the medullary respiratory chemoreceptors and pulmonary stretch receptors (Gaytan and Pasaro, 1998; Hanamori et al., 1998). Stimulation studies of the vagus nerve and the insula have demonstrated reciprocal respiratory projections in humans and other mammals (Kaada, 1951; Radna and MacLean, 1981). Notably, electrical stimulation of the anterior insular cortex has been consistently demonstrated to have strong inhibitory effects on respiration (e.g., apnea) (Hoffman and Rasmussen, 1953; Kaada and Jasper, 1952).

Given the preceding evidence, the insula would also be well connected to mediate changes in breathing. Yet, no significant differential insular activity was observed for the RNG > BASE (or RNG < BASE) interaction(s), suggesting a lack of insular modulation of respiratory rate during the cognitive task. It is noteworthy that breath-by-breath synchronization with the BOLD signal was observed in two functionally distinct locations, the right anterior insula and the left posterior insula. The posterior insula has been implicated in autonomic/homeostatic function (Craig, 2009; Critchley et al., 2000; Napadow et al., 2008). While our interaction analyses failed to demonstrate differential insular activity correlated with breathing, the independent condition analyses suggest the left posterior insular activity was present in the RNG condition but not the BASE condition (Supplementary Table 2). In line with findings in rodents (Aleksandrov et al., 2000), we speculate that the posterior insula may contribute to efferent processes underlying the increased respiratory frequency associated with the cognitive task. However, we view this consideration with great caution as a positive posterior insula finding for the interaction analyses would have been indisputably more convincing.

We consider our right anterior insula findings as holding greater strength (over the left posterior insula finding) as comparable right anterior insular activity was associated with breathing for the main effects (RNG + BASE) (Table 2, Figure 2) and for both RNG and BASE conditions considered separately (Supplementary Table 2). Collectively, these right anterior insular findings from the present study are comparable to those reported in our earlier study of dyspnea (Evans et al., 2002). Interestingly, activation of the anterior insula has been the most consistent limbic/paralimbic finding across all published neuroimaging studies of laboratory induced dyspnea (Banzett et al., 2000; Brannan et al., 2001; Evans et al., 2002; Peiffer et al., 2001; von Leupoldt et al., 2008). The anterior insula has also been implicated in breath awareness (Lazar et al., 2005) as well as several other primitive, interoceptive processes such as pain, thirst and hunger (Craig, 2002; Denton, 2005; Denton et al., 1999; Tataranni et al., 1999; Tracey and Mantyh, 2007). Consequently we propose that the breath-by-breath synchronization of BOLD signal within the anterior insular loci represents afferent activity related to breathing. Future studies are needed to confirm the role of the insula in spontaneous breathing.

Brainstem

The main effects of condition analysis demonstrated distinct regional activity synchronized with the respiratory cycle within separate circumscribed loci at all three levels of the brainstem (midbrain, pons and medulla). Modulation of this activity was observed within key centers of respiratory control. Several earlier neuroimaging studies have demonstrated

regional brainstem activity but only via contrasts of significant respiratory perturbation (e.g., hyperpnea, hypercapnia, hypoxia, loaded breathing, and breath-hold) (Gozal et al., 1995; Harper et al., 2005; Liotti et al., 2001; Macey et al., 2004; Macey et al., 2005; McKay et al., 2008; McKay et al., 2003; Pattinson et al., 2009). The present study is the first to identify respiratory related brainstem activity during unlabored waking breathing, and first to demonstrate modulation in brainstem activity associated with increased breathing frequency provoked by a cognitive task.

The main effects of condition (RNG + BASE) (Table 2, Figure 1) and independent condition analyses (Supplementary table 2) all shared comparable regional activity localized to the medulla and rostral pons. The medullary activity spanned from *z*-plane −54 to −60, and localized centrally. The medullary activity was consistent with previous findings during hyperpnea (McKay et al., 2003) and the recent findings of Pattinson and colleagues during hypercapnia (Pattinson et al., 2009). The rostral pontine activity observed in the main effects spanned from *z*-plane −30 to −32 and was distributed among a central cluster localized to the paramedian raphe, to bilateral satellite clusters extending dorsally and laterally to the Kölliker–Fuse (KF) nuclei and adjoining parabrachial (PB) nuclei and locus coeruleus (Figure 1). The resolution of fMRI at 1.5 Tesla precludes the differentiation of these essentially overlapping nuclei. Following the classic convention, we consider them here together as the KF/PB complex. The main effects activity localized to the KF/PB complex shared similar localization with KF/PB complex findings in the hypercapnia study of Pattinson and colleagues (2009) and the neuroimaging study of volitional breath-hold of McKay and colleagues (2008). Taken together, the present finding of combined medullary and KF/PB complex activity that is synchronized with the respiratory cycle is in accord with contemporary theories that purport dynamic network activity between these structures drives the intrinsic brainstem respiratory rhythm (Alheid et al., 2004; Rybak et al., 2004). Anterograde and retrograde tract tracing studies in animals provide support for this interaction as the brainstem respiratory centers have been shown to be densely interconnected (Gaytan and Pasaro, 1998; Lois et al., 2008; Ricardo and Koh, 1978).

Significant main effects were also observed in the midbrain. As reviewed by Horn and Waldrop (1998) the midbrain receives input from the limbic system and projects to brainstem respiratory nuclei (e.g., NTS, KF/PB complex). The midbrain is also known to receive afferent projections from pulmonary stretch receptors as well as the nasal skin and mucosa independently from ascending medullary input (Chen and Eldridge, 1997). Animal stimulation studies have shown midbrain influence over phrenic nerve as well as medullary respiratory neurons (Schmid et al., 1988). Midbrain findings in neuroimaging studies have been inconsistent. Significant midbrain activity was reported in studies that employed respiratory resistive loads (Fink et al., 1996; Gozal et al., 1995), in accord with animal studies (Eldridge and Chen, 1992). However, significant midbrain activity was not reported in a previous neuroimaging study of hyperpnea (McKay et al., 2003), nor in recent neuroimaging studies of breath-hold (McKay et al., 2008) and hypercapnia (Pattinson et al., 2009) (but see Liotti et al.(2001)). Taken together, we propose methodological issues have contributed to the disparate midbrain findings in the neuroimaging literature. We further propose that the breath-by-breath analytic method employed in the present study may have conferred enhanced sensitivity to identify activity in a region that had only previously been seen in studies of hypercapnia and resistive loading. We suggest our midbrain finding reflects essential involvement of the mesencephalon in resting spontaneous breathing.

Robust ventral pontine activity was identified in the interaction analysis (RNG > BASE), localized to the midline raphe magnus nucleus, extending dorsally and laterally to the raphe interpositus and gigantocellular reticularis nucleus with a span from *z*-plane −41 to −51. (Table 2, Figure 3). The magnus raphe is known to have connections with other important

brainstem respiratory centers, namely the solitary tract nucleus, Botzinger complex, retrotrapezoidal nucleus and KF/PB complex (Gang et al., 1995; Hermann et al., 1997). Projections from the raphe magnus to the C4 phrenic nerve segments have been identified in studies of spontaneously breathing rodents (Hosogai et al., 1998). In addition to important intra-brainstem and phrenic connections, the raphe magnus is known to have projections to the midbrain reticular formation, the central nucleus of the amygdala and the insula. Further, the raphe magnus is known to be one of the few serotonergic centers in the brainstem and appears to have highly specific respiratory function (Mason et al., 2007) and coordinated respiratory/cardiovascular function (Messier and Nattie, 2004). Ventral pontine activity in the vicinity of the raphe magnus identified by the current study has also been recently reported in the neuroimaging study of hypercapnia by Pattinson and colleagues (2009) and the breath-hold study of McKay and colleagues (2008). Given this convergence of findings together with the raphe magnus profile of connectivity, neurotransmission and respiratory specificity, we propose that the differential raphe magnus activity (RNG > BASE) serves in part (perhaps in coordination with the dACC via polysynaptic connection) to mediate the increased f_R during the RNG condition.

Post hoc findings

Several *post hoc* findings met the significance threshold for whole brain volume search (FWE, $P < 0.05$, corrected for multiple comparisons). As noted, we present the *post-hoc* results in Supplemental Table 2 in order to illustrate the specificity of the predicted findings and for completeness. The subthalamic nucleus was a robust yet unexpected finding that may have implications for future studies given its connections to limbic/paralimbic-bulbar circuitry and its known multimodal roles in emotional and motor processing (Gaytan and Pasaro, 1998; Mallet et al., 2007). Several other prominent post hoc findings included respiratory related activity within the classical motor areas (e.g., putamen) as well as temporal and occipital regions. Temporal lobe findings (outside of limbic/paralimbic circuitry) associated with respiration have been common and will require future studies for determining their functional significance. (Kaada and Jasper, 1952; Loucks et al., 2007; Masaoka et al., 2003; Simonyan et al., 2007).

Limitations

Interpretations of the present study should be considered in the context of acknowledged limitations. The present study considered both full brain and small volume corrected image analyses. Given the strong a priori hypotheses this was deemed appropriate for this first ever breath-by-breath, event-related fMRI study of unlabored spontaneous breathing, emphasizing the necessity of future studies to assess the reproducibility and generalizability of the present findings. Further, the present study like most all studies of respiration physiology required subjects to breathe through ventilatory monitoring equipment, which compared to ‘natural’ unimpeded breathing, is known to influence respiratory variables (Han et al., 1997; Shea, 1996; Tobin et al., 1983). Explanations for experimentally induced changes in breathing include: increased dead space (3.9 ml in the present study), changes in upper airway resistance and unintended attentional focus on breathing. We can not exclude the possibility that the subjects were more focused on their breathing during the BASE condition (in the absence of the demanding cognitive task). In short of adequate objective measures of task performance, attention or autonomic arousal (beyond heart rate, which was unchanged) it was not possible to quantify the contribution of such bias on the observed between condition effects. The lack of measures of task performance also precluded confirmation that each subject actually performed RNG as instructed. However, the significantly increased respiratory rate during the RNG condition, relative to the BASE condition, is highly suggestive that the subjects were engaged in more demanding mental activity during the RNG condition (Mador and Tobin, 1991; Shea, 1996; Shea et al., 1987).

The BOLD-fMRI signal is known to be susceptible to several common sources of variance such as head-movement and artifacts introduced by respiration (Birn et al., 2006; Kastrup et al., 1999). Respiration-related artifacts have been attributed to: 1) fluctuations in PCO_2, which lead to changes in cerebral vasculature dilation and subsequent changes in cerebral blood flow, 2) lung and chest-wall movement during the respiratory cycle that can induce shifts in the magnetic field. In the present study, we corrected for movement-related sources of variance during image pre-processing with advanced realignment and unwarping algorithms now standard in SPM5. Notably the unwarping algorithms correct for "movement by distortion" interactions in regions with prominent air-tissue interface that are most susceptible to geometric distortions, such as the medial temporal lobe and brainstem (for details see http://www.fil.ion.ucl.ac.uk/spm/doc/manual.pdf). To further correct for the potential effects of movement-related variance that persisted after pre-processing, we included the realignment parameters as null regressors in our analytic models as this approach has been shown to enhance neural signal detection (Lund et al., 2005), particularly in subcortical structures (Friston et al., 1996). However this approach carries a susceptibility to Type II error, specifically, the exclusion of respiratory-related movement renders the possibility of excluding regional BOLD signal changes driven by respiratory-related neural activity within limbic/paralimbic and brainstem circuitry. We thus view this approach as highly conservative. Our use of two independent analytic approaches to account for physiological noise (i.e., the global regressor and the PCO_2 regressor) can be considered similarly conservative. We contend the global regressor approach is exceedingly conservative (see Birn, et al., 2006) and thus made the *a priori* decision the report our primary findings from the global regressor analysis. The secondary findings from the PCO_2 regressor analysis confirmed the primary findings. Both approaches have susceptibility to Type II error, yet the advantage of their use is underscored by the validated ability to detect "real" neural signals while avoiding Type I error in experimental conditions where PCO_2 could have otherwise served as a major confound (Corfield et al., 2001; Wise et al., 2004). Since the initiation of the present study, other relevant studies have reported on novel methods to address these very issues (Birn et al., 2006; Harvey, 2008). Despite the recent developments in this realm, we contend that the inclusion of both realignment parameters and global signal as null regressors in our primary analytic models served as an effective strategy in avoiding Type I errors. Efficacy for the regressor approach has been previously demonstrated in several other studies of respiration (Evans et al., 2002; McKay et al., 2003; von Leupoldt et al., 2008). Notably using this same approach robust cortical, subcortical and circumscribed brainstem medullary activity was identified during a hyperpnea task (McKay et al., 2003) and similarly robust findings were observed during a study of breath-hold (McKay et al., 2008). Lastly, the peri-event time courses (Figure 3.) provide support for the observed between condition effects where BOLD signal peaked within 4–8 sec, consistent with the canonical hemodynamic response function (HRF) associated with neural activity. Whereas BOLD artifacts related to respiration have been shown have significant latency, inconsistent with the canonical HRF (Birn et al., 2008).

Summary

Limbic influences on breathing are poorly understood and have served to generate scientific curiosity for decades. During waking breathing limbic and paralimbic brain regions have been postulated to modulate the fundamental respiratory pattern established by the brainstem pacemaker neurons. While lesion, electrical stimulation and limited *in vivo* recording studies in patient populations and animal models have implicated several limbic/paralimbic regions in the control of breathing, a putative network of limbic/paralimbic regions involved in unanesthetized, spontaneously breathing in healthy individuals had yet to be delineated. In the present study we demonstrated the first evidence of synchronized neural activity across a distributed network of limbic/paralimbic and brainstem elements during unlabored

spontaneous breathing. We have further demonstrated that the imposition of a simple cognitive task produced expected increased breathing rate and marked modulation of neuronal activity within this network localized to the pontine raphe magnus, amygdala and anterior cingulate cortex. These findings suggest the identified limbic/paralimbic-bulbar circuitry plays a significant role in resting spontaneous breathing, as well as in mediating cognitive influences on breathing. Future studies will be required to further elucidate the role of these loci under other conditions, such as emotional provocation. We anticipate the present findings will have implications for investigators from wide-reaching disciplines, including pulmonary medicine, neurology, psychiatry, and mind-body medicine.

Supplementary Material

Refer to Web version on PubMed Central for supplementary material.

Acknowledgments

We wish to acknowledge Randy Buckner, Robert Banzett and Kenneth Kwong for their thoughtful discussion and comments. This work was supported in part by grants H75/CCH119124, H75/CCH123424 and 5R01DP000339. Dr. Evans received support from grants T-32 EB001632-03 (NIBIB), R21 AT003425-01A2S1 (NCCAM) and a Faculty Development Award from the Massachusetts General Hospital Executive Committee on Research. Dr. Lazar received support from grants K01AT00694-01 (NCCAM) and 1R21AT003673-01 (NCCAM).

References

Aleksandrov VG, Aleksandrova NP, Bagaev VA. Identification of a respiratory related area in the rat insular cortex. Can J Physiol Pharmacol. 2000; 78(7):582–586. [PubMed: 10926166]

Alheid GF, Milsom WK, McCrimmon DR. Pontine influences on breathing: an overview. Respir Physiol Neurobiol. 2004; 143(2–3):105–114. [PubMed: 15519548]

Augustine JR. Circuitry and functional aspects of the insular lobe in primates including humans. Brain Research Reviews. 1996; 22:229–244. [PubMed: 8957561]

Banzett RB, Mulnier HE, Murphy K, Rosen SD, Wise RJ, Adams L. Breathlessness in humans activates insular cortex. Neuroreport. 2000; 11(10):2117–2120. [PubMed: 10923655]

Bendixen HH, Smith C, Mend J. Pattern of ventilation in young adults. J Appl Physiol. 1964; 19:195–198. [PubMed: 14155280]

Birn RM, Diamond JB, Smith MA, Bandettini PA. Separating respiratory-variation-related fluctuations from neuronal-activity-related fluctuations in fMRI. Neuroimage. 2006; 31(4):1536–1548. [PubMed: 16632379]

Birn RM, Smith MA, Jones TB, Bandettini PA. The respiration response function: the temporal dynamics of fMRI signal fluctuations related to changes in respiration. Neuroimage. 2008; 40(2): 644–654. [PubMed: 18234517]

Boiten FA. The effects of emotional behaviour on components of the respiratory cycle. Biol Psychol. 1998; 49(1–2):29–51. [PubMed: 9792483]

Bonvallet M, Bobo EG. Changes in phrenic activity and heart rate elicited by localized stimulation of amygdala and adjacent structures. Electroencephalogr Clin Neurophysiol. 1972; 32(1):1–16. [PubMed: 4109912]

Brannan S, Liotti M, Egan G, Shade R, Madden L, Robillard R, Abplanalp B, Stofer K, Denton D, Fox PT. Neuroimaging of cerebral activations and deactivations associated with hypercapnia and hunger for air. Proc Natl Acad Sci U S A. 2001; 98(4):2029–2034. [PubMed: 11172070]

Buchanan SL, Thompson RH, Maxwell BL, Powell DA. Efferent connections of the medial prefrontal cortex in the rabbit. Exp Brain Res. 1994; 100(3):469–483. [PubMed: 7529194]

Bush G, Luu P, Posner MI. Cognitive and emotional influences in anterior cingulate cortex. Trends Cogn Sci. 2000; 4(6):215–222. [PubMed: 10827444]

Chen Z, Eldridge FL. Inputs from upper airway affect firing of respiratory-associated midbrain neurons. J Appl Physiol. 1997; 83(1):196–203. [PubMed: 9216964]

Colebatch JG, Adams L, Murphy K, Martin AJ, Lammertsma AA, Tochon-Danguy HJ, Clark JC, Friston KJ, Guz A. Regional cerebral blood flow during volitional breathing in man. J Physiol. 1991; 443:91–103. [PubMed: 1822545]

Corfield DR, Murphy K, Josephs O, Adams L, Turner R. Does hypercapniainduced cerebral vasodilation modulate the hemodynamic response to neural activation? Neuroimage. 2001; 13(6 Pt 1):1207–1211. [PubMed: 11352626]

Craig AD. How do you feel? Interoception: the sense of the physiological condition of the body. Nature Neurosci. 2002; 3:655–666.

Craig AD. How do you feel--now? The anterior insula and human awareness. Nat Rev Neurosci. 2009; 10(1):59–70. [PubMed: 19096369]

Critchley HD, Corfield DR, Chandler MP, Mathias CJ, Dolan RJ. Cerebral correlates of autonomic cardiovascular arousal: a functional neuroimaging investigation in humans. J Physiol. 2000; 523(Pt 1):259–270. [PubMed: 10673560]

Dale AM. Optimal experimental design for event-related fMRI. Hum Brain Mapp. 1999; 8(2–3):109–114. [PubMed: 10524601]

Denton, D. The Primordial Emotions: The dawning of consciousness. New York: Oxford University Press; 2005.

Denton D, Shade R, Zamarippa F, Egan G, Blair-West J, McKinley M, Fox P. Correlation of regional cerebral blood flow and change of plasma sodium concentration during genesis and satiation of thirst. Proceedings National Academy of Science. 1999; 96:2532–2537.

Duvernoy, H. Surface, three dimensional sectional anatomy with MRI, and blood supply. New York: Springer-Wien; 1999. The Human Brain.

Eldridge FL, Chen Z. Respiratory-associated rhythmic firing of midbrain neurons is modulated by vagal input. Respiration Physiology. 1992; 90(1):31–46. [PubMed: 1455097]

Evans KC, Banzett RB, Adams L, McKay L, Frackowiak RS, Corfield DR. BOLD fMRI identifies limbic, paralimbic, and cerebellar activation during air hunger. J Neurophysiol. 2002; 88(3):1500–1511. [PubMed: 12205170]

Evans KC, Shea SA, Saykin AJ. Functional MRI localisation of central nervous system regions associated with volitional inspiration in humans. J Physiol. 1999; 520(Pt 2):383–392. [PubMed: 10523407]

Feldman JL, Del Negro CA. Looking for inspiration: new perspectives on respiratory rhythm. Nat Rev Neurosci. 2006; 7(3):232–242. [PubMed: 16495944]

Filipek PA, Richelme C, Kennedy DN, Caviness VS Jr. The young adult human brain: an MRI-based morphometric analysis. Cereb Cortex. 1994; 4(4):344–360. [PubMed: 7950308]

Fink BR. Influence of cerebral activity in wakefulness on regulation of breathing. J Appl Physiol. 1961; 16:15–20. [PubMed: 13699604]

Fink GR, Corfield DR, Murphy K, Kobayashi I, Dettmers C, Adams L, Frackowiak RS, Guz A. Human cerebral activity with increasing inspiratory force: a study using positron emission tomography. J Appl Physiol. 1996; 81(3):1295–1305. [PubMed: 8889766]

Foerster, O. Handbuch der Neurologie. Berlin, Germany: Springer; 1936.

Friston, KJ.; Ashburner, J.; Kiebel, SJ.; Nichols, TE.; Penny, WD. Statistical parametric mapping the analysis of functional brain images. London: Academic Press; 2007.

Friston KJ, Williams S, Howard R, Frackowiak RS, Turner R. Movement-related effects in fMRI time-series. Magn Reson Med. 1996; 35(3):346–355. [PubMed: 8699946]

Frysinger RC, Harper RM. Cardiac and respiratory correlations with unit discharge in human amygdala and hippocampus. Electroencephalogr Clin Neurophysiol. 1989; 72(6):463–470. [PubMed: 2471614]

Frysinger RC, Harper RM. Cardiac and respiratory correlations with unit discharge in epileptic human temporal lobe. Epilepsia. 1990; 31(2):162–171. [PubMed: 2318169]

Gabbott PL, Warner TA, Jays PR, Salway P, Busby SJ. Prefrontal cortex in the rat: projections to subcortical autonomic, motor, and limbic centers. J Comp Neurol. 2005; 492(2):145–177. [PubMed: 16196030]

Gang S, Sato Y, Kohama I, Aoki M. Afferent projections to the Botzinger complex from the upper cervical cord and other respiratory related structures in the brainstem in cats: retrograde WGA-HRP tracing. J Auton Nerv Syst. 1995; 56(1–2):1–7. [PubMed: 8786271]

Gaytan SP, Pasaro R. Connections of the rostral ventral respiratory neuronal cell group: an anterograde and retrograde tracing study in the rat. Brain Res Bull. 1998; 47(6):625–642. [PubMed: 10078619]

Gozal D, Omidvar O, Kirlew KA, Hathout GM, Hamilton R, Lufkin RB, Harper RM. Identification of human brain regions underlying responses to resistive inspiratory loading with functional magnetic resonance imaging. Proc Natl Acad Sci U S A. 1995; 92(14):6607–6611. [PubMed: 7604040]

Grossman P. Respiration, stress, and cardiovascular function. Psychophysiology. 1983; 20(3):284–300. [PubMed: 6408680]

Guz A. Brain, breathing and breathlessness. Resp Physiol. 1997; 109:197–204.

Halgren E, Babb TL, Crandall PH. Responses of human limbic neurons to induced changes in blood gases. Brain Res. 1977; 132(1):43–63. [PubMed: 19127]

Han JN, Stegen K, Cauberghs M, Van de Woestijne KP. Influence of awareness of the recording of breathing on respiratory pattern in healthy humans. Eur Respir J. 1997; 10(1):161–166. [PubMed: 9032510]

Hanamori T, Kunitake T, Kato K, Kannan H. Neurons in the posterior insular cortex are responsive to gustatory stimulation of the pharyngolarynx, baroreceptor and chemoreceptor stimulation, and tail pinch in rats. Brain Res. 1998; 785(1):97–106. [PubMed: 9526057]

Harper RM, Macey PM, Woo MA, Macey KE, Keens TG, Gozal D, Alger JR. Hypercapnic exposure in congenital central hypoventilation syndrome reveals CNS respiratory control mechanisms. J Neurophysiol. 2005; 93(3):1647–1658. [PubMed: 15525806]

Harvey AK, Pattinson KTS, Brooks JCW, Mayhew SD, Jenkinson M, Wise RG. Brainstem Functional Magnetic Resonance Imaging: Disentangling Signal From Physiological Noise. J Magn Reson Imaging. 2008:28.

Hatanaka N, Tokuno H, Hamada I, Inase M, Ito Y, Imanishi M, Hasegawa N, Akazawa T, Nambu A, Takada M. Thalamocortical and intracortical connections of monkey cingulate motor areas. J Comp Neurol. 2003; 462(1):121–138. [PubMed: 12761828]

Hermann DM, Luppi PH, Peyron C, Hinckel P, Jouvet M. Afferent projections to the rat nuclei raphe magnus, raphe pallidus and reticularis gigantocellularis pars alpha demonstrated by iontophoretic application of choleratoxin (subunit b). J Chem Neuroanat. 1997; 13(1):1–21. [PubMed: 9271192]

Hoffman BL, Rasmussen T. Stimulation studies of insular cortex of macaca mulatta. J Neurophysiol. 1953; 16:343–350. [PubMed: 13070046]

Homma I, Masaoka Y. Breathing rhythms and emotions. Exp Physiol. 2008; 93(9):1011–1021. [PubMed: 18487316]

Horn EM, Waldrop TG. Suprapontine control of respiration. Respir Physiol. 1998; 114(3):201–211. [PubMed: 9926985]

Hosogai M, Matsuo S, Sibahara T, Kawai Y. Projection of respiratory neurons in rat medullary raphe nuclei to the phrenic nucleus. Respir Physiol. 1998; 112(1):37–50. [PubMed: 9696281]

Hugelin, A. Forebrain and midbrain influence on respiration. In: Cherniack, NS.; Widdicombe, JG., editors. Handbook of Physiology, Sect. 3: The respiratory System. Bethesda: American Physiological Society; 1986.

Kaada BR. Somato-motor, autonomic and electrocorticographic responses to electrical stimulation of rhinencephalic and other structures in primates, cat and dog. Acta Physiologica Scandinavica. 1951; 24(suppl 83):1–285. [PubMed: 14877579]

Kaada BR, Jasper H. Respiratory responses to stimulation of temporal pole, insula, and hippocampal and limbic gyri in man. AMA Arch Neurol Psychiatry. 1952; 68(5):609–619.

Kastrup A, Kruger G, Glover GH, Neumann-Haefelin T, Moseley ME. Regional variability of cerebral blood oxygenation response to hypercapnia. Neuroimage. 1999; 10(6):675–681. [PubMed: 10600413]

Kennedy DN, Lange N, Makris N, Bates J, Meyer J, Caviness VS Jr. Gyri of the human neocortex: an MRI-based analysis of volume and variance. Cereb Cortex. 1998; 8(4):372–384. [PubMed: 9651132]

Kremer WF. Autonomic and somatic reactions induced by stimulation of the cingular gyrus in dogs. J Neurophysiol. 1947; 10:371–379. [PubMed: 20265864]

Lazar SW, Kerr CE, Wasserman RH, Gray JR, Greve DN, Treadway MT, McGarvey M, Quinn BT, Dusek JA, Benson H, Rauch SL, Moore CI, Fischl B. Meditation experience is associated with increased cortical thickness. Neuroreport. 2005; 16(17):1893–1897. [PubMed: 16272874]

LeDoux JE. Emotion circuits in the brain. Annu Rev Neurosci. 2000; 23:155–184. [PubMed: 10845062]

Liotti M, Brannan S, Egan G, Shade R, Madden L, Abplanalp B, Robillard R, Lancaster J, Zamarripa FE, Fox PT, Denton D. Brain responses associated with consciousness of breathlessness (air hunger). Proc Natl Acad Sci U S A. 2001; 98(4):2035–2040. [PubMed: 11172071]

Lois JH, Rice CD, Yates BJ. Neural Circuits Controlling Diaphragm Function in the Cat Revealed by Transneuronal Tracing. J Appl Physiol. 2008

Loucks TM, Poletto CJ, Simonyan K, Reynolds CL, Ludlow CL. Human brain activation during phonation and exhalation: common volitional control for two upper airway functions. Neuroimage. 2007; 36(1):131–143. [PubMed: 17428683]

Luft AR, Skalej M, Schulz JB, Welte D, Kolb R, Burk K, Klockgether T, Voight K. Patterns of age-related shrinkage in cerebellum and brainstem observed in vivo using three-dimensional MRI volumetry. Cereb Cortex. 1999; 9(7):712–721. [PubMed: 10554994]

Lumsden T. Observations on the respiratory centres. J Physiol. 1923; 57(6):354–367. [PubMed: 16993579]

Lund TE, Norgaard MD, Rostrup E, Rowe JB, Paulson OB. Motion or activity: their role in intra- and inter-subject variation in fMRI. Neuroimage. 2005; 26(3):960–964. [PubMed: 15955506]

Macefield VG, Gandevia SC, Henderson LA. Neural sites involved in the sustained increase in muscle sympathetic nerve activity induced by inspiratory capacity apnea: a fMRI study. J Appl Physiol. 2006; 100(1):266–273. [PubMed: 16123207]

Macey KE, Macey PM, Woo MA, Harper RK, Alger JR, Keens TG, Harper RM. fMRI signal changes in response to forced expiratory loading in congenital central hypoventilation syndrome. J Appl Physiol. 2004; 97(5):1897–1907. [PubMed: 15258126]

Macey PM, Woo MA, Macey KE, Keens TG, Saeed MM, Alger JR, Harper RM. Hypoxia reveals posterior thalamic, cerebellar, midbrain, and limbic deficits in congenital central hypoventilation syndrome. J Appl Physiol. 2005; 98(3):958–969. [PubMed: 15531561]

Mador MJ, Tobin MJ. Effect of alterations in mental activity on the breathing pattern in healthy subjects. Am Rev Respir Dis. 1991; 144(3 Pt 1):481–487. [PubMed: 1892283]

Mai, JK.; Assheuer, J.; Paxinos, G. Atlas of the Human Brain. London: Academic Press, Ltd; 1997.

Makris N, Goldstein JM, Kennedy D, Hodge SM, Caviness VS, Faraone SV, Tsuang MT, Seidman LJ. Decreased volume of left and total anterior insular lobule in schizophrenia. Schizophr Res. 2006; 83(2–3):155–171. [PubMed: 16448806]

Maldjian JA, Laurienti PJ, Kraft RA, Burdette JH. An automated method for neuroanatomic and cytoarchitectonic atlas-based interrogation of fMRI data sets. Neuroimage. 2003; 19(3):1233–1239. [PubMed: 12880848]

Mallet L, Schupbach M, N'Diaye K, Remy P, Bardinet E, Czernecki V, Welter ML, Pelissolo A, Ruberg M, Agid Y, Yelnik J. Stimulation of subterritories of the subthalamic nucleus reveals its role in the integration of the emotional and motor aspects of behavior. Proc Natl Acad Sci U S A. 2007; 104(25):10661–10666. [PubMed: 17556546]

Marchand JE, Hagino N. Afferents to the periaqueductal gray in the rat. A horseradish peroxidase study. Neuroscience. 1983; 9(1):95–106. [PubMed: 6877597]

Masaoka Y, Hirasawa K, Yamane F, Hori T, Homma I. Effects of left amygdala lesions on respiration, skin conductance, heart rate, anxiety, and activity of the right amygdala during anticipation of negative stimulus. Behav Modif. 2003; 27(5):607–619. [PubMed: 14531157]

Masaoka Y, Homma I. Anxiety and respiratory patterns: their relationship during mental stress and physical load. Int J Psychophysiol. 1997; 27(2):153–159. [PubMed: 9342646]

Masaoka Y, Homma I. The source generator of respiratory-related anxiety potential in the human brain. Neurosci Lett. 2000; 283(1):21–24. [PubMed: 10729624]

Mason P, Gao K, Genzen JR. Serotonergic raphe magnus cell discharge reflects ongoing autonomic and respiratory activities. J Neurophysiol. 2007; 98(4):1919–1927. [PubMed: 17715191]

Mazzone SB, McLennan L, McGovern AE, Egan GF, Farrell MJ. Representation of capsaicin-evoked urge-to-cough in the human brain using functional magnetic resonance imaging. Am J Respir Crit Care Med. 2007; 176(4):327–332. [PubMed: 17575093]

McKay LC, Adams L, Frackowiak RS, Corfield DR. A bilateral cortico-bulbar network associated with breath holding in humans, determined by functional magnetic resonance imaging. Neuroimage. 2008; 40(4):1824–1832. [PubMed: 18343687]

McKay LC, Evans KC, Frackowiak RS, Corfield DR. Neural correlates of voluntary breathing in humans. J Appl Physiol. 2003; 95(3):1170–1178. [PubMed: 12754178]

Mechelli A, Henson RN, Price CJ, Friston KJ. Comparing event-related and epoch analysis in blocked design fMRI. Neuroimage. 2003; 18(3):806–810. [PubMed: 12667857]

Messier ML, Nattie E. Inhibition of medullary raphe serotonergic neurons has age-dependent effects on the CO2 response in newborn piglets. J Appl Physiol. 2004; 96(5):1909–1919. [PubMed: 14752121]

Mesulam MM, Mufson EJ. Insula of the old world monkey. III: Efferent cortical output and comments on function. J Comp Neurol. 1982; 212(1):38–52. [PubMed: 7174907]

Miezin FM, Maccotta L, Ollinger JM, Petersen SE, Buckner RL. Characterizing the hemodynamic response: effects of presentation rate, sampling procedure, and the possibility of ordering brain activity based on relative timing. Neuroimage. 2000; 11(6 Pt 1):735–759. [PubMed: 10860799]

Mitchell, RA.; Berger, AJ. Neural Regulation of Respiration. In: Hornbein, TF., editor. Regulation of Breathing: Part I. New York: Marcel Dekker, Inc; 1981. p. 541-620.

Mufson EJ, Mesulam MM. Insula of the old world monkey. II: Afferent cortical input and comments on the claustrum. J Comp Neurol. 1982; 212(1):23–37. [PubMed: 7174906]

Napadow V, Dhond R, Conti G, Makris N, Brown EN, Barbieri R. Brain correlates of autonomic modulation: Combining heart rate variability with fMRI. Neuroimage. 2008; 42(1):169–177. [PubMed: 18524629]

Onimaru H, Homma I. Spontaneous oscillatory burst activity in the piriform-amygdala region and its relation to in vitro respiratory activity in newborn rats. Neuroscience. 2007; 144(1):387–394. [PubMed: 17074446]

Papp LA, Martinez JM, Klein DF, Coplan JD, Norman RG, Cole R, de Jesus MJ, Ross D, Goetz R, Gorman JM. Respiratory psychophysiology of panic disorder: three respiratory challenges in 98 subjects. Am J Psychiatry. 1997; 154(11):1557–1565. [PubMed: 9356564]

Pattinson KT, Mitsis GD, Harvey AK, Jbabdi S, Dirckx S, Mayhew SD, Rogers R, Tracey I, Wise RG. Determination of the human brainstem respiratory control network and its cortical connections in vivo using functional and structural imaging. Neuroimage. 2009; 44(2):295–305. [PubMed: 18926913]

Paxinos, G.; Huang, X-F. Atlas of the Human Brainstem. San Diego: Academic Press Inc; 1995.

Peiffer C, Poline JB, Thivard L, Aubier M, Samson Y. Neural substrates for the perception of acutely induced dyspnea. Am J Respir Crit Care Med. 2001; 163(4):951–957. [PubMed: 11282772]

Penfield W, Faulk ME Jr. The insula; further observations on its function. Brain. 1955; 78(4):445–470. [PubMed: 13293263]

Pool JL, Ransohoff J. Autonomic effects on stimulating rostral portion of cingulate gyri in man. J Neurophysiol. 1949; 6:385–92. [PubMed: 15408005]

Priban IP. An analysis of some short-term patterns of breathing in man at rest. J Physiol. 1963; 166:425–434. [PubMed: 13986111]

Radna RJ, MacLean PD. Vagal elicitation of respiratory-type and other unit responses in basal limbic structures of squirrel monkeys. Brain Res. 1981; 213(1):45–61. [PubMed: 7237150]

Ramsay SC, Adams L, Murphy K, Corfield DR, Grootoonk S, Bailey DL, Frackowiak RS, Guz A. Regional cerebral blood flow during volitional expiration in man: a comparison with volitional inspiration. J Physiol. 1993; 461:85–101. [PubMed: 8350282]

Ricardo JA, Koh ET. Anatomical evidence of direct projections from the nucleus of the solitary tract to the hypothalamus, amygdala, and other forebrain structures in the rat. Brain Res. 1978; 153(1):1–26. [PubMed: 679038]

Rybak IA, Shevtsova NA, Paton JF, Dick TE, St-John WM, Morschel M, Dutschmann M. Modeling the ponto-medullary respiratory network. Respir Physiol Neurobiol. 2004; 143(2–3):307–319. [PubMed: 15519563]

Schmid K, Bohmer G, Fallert M. Influence of rubrospinal tract and the adjacent mesencephalic reticular formation on the activity of medullary respiratory neurons and the phrenic nerve discharge in the rabbit. Pflugers Arch. 1988; 413(1):23–31. [PubMed: 3217224]

Shea SA. Behavioural and arousal-related influences on breathing in humans. Exp Physiol. 1996; 81(1):1–26. [PubMed: 8869137]

Shea SA, Walter J, Pelley C, Murphy K, Guz A. The effect of visual and auditory stimuli upon resting ventilation in man. Respir Physiol. 1987; 68(3):345–357. [PubMed: 3616180]

Shi CJ, Cassell MD. Cortical, thalamic, and amygdaloid connections of the anterior and posterior insular cortices. J Comp Neurol. 1998; 399(4):440–468. [PubMed: 9741477]

Simonyan K, Saad ZS, Loucks TM, Poletto CJ, Ludlow CL. Functional neuroanatomy of human voluntary cough and sniff production. Neuroimage. 2007; 37(2):401–409. [PubMed: 17574873]

Speakman TJ, Babkin BP. Effect of cortical stimulation on respiratory rate. Am J Physiol. 1949; 159(2):239–246. [PubMed: 15407003]

Spencer WG. The Effect produced upon respiration by faradic excitationof the cerebrum in the monkey, dog, and cat. Philos Trans R Soc Lond B Biol Sci. 1896; B185:609–657.

St John WM, Paton JF. Role of pontile mechanisms in the neurogenesis of eupnea. Respir Physiol Neurobiol. 2004; 143(2–3):321–332. [PubMed: 15519564]

Talairach, J.; Tournoux, P. Coplanar stereotaxic atlas of the human brain. Stuttgart: Thieme; 1988.

Tataranni PA, Gautier J-F, Chen K, Uecker A, Bandy D, Salbe AD, Pratley RE, Lawson M, Reiman EM, Ravussin E. Neuroanatomical correlates of hunger and satiation in humans using positron emission tomography. Proceedings of the National Academy of Science. 1999; 96:4569–4574.

Tobin MJ, Chadha TS, Jenouri G, Birch SJ, Gazeroglu HB, Sackner MA. Breathing patterns. 1. Normal subjects. Chest. 1983; 84(2):202–205. [PubMed: 6872603]

Tobin MJ, Mador MJ, Guenther SM, Lodato RF, Sackner MA. Variability of resting respiratory drive and timing in healthy subjects. J Appl Physiol. 1988; 65(1):309–317. [PubMed: 3403474]

Tracey I, Mantyh PW. The cerebral signature for pain perception and its modulation. Neuron. 2007; 55(3):377–391. [PubMed: 17678852]

Tsumori T, Yokota S, Kishi T, Qin Y, Oka T, Yasui Y. Insular cortical and amygdaloid fibers are in contact with posterolateral hypothalamic neurons projecting to the nucleus of the solitary tract in the rat. Brain Res. 2006; 1070(1):139–144. [PubMed: 16388783]

Tzourio-Mazoyer N, Landeau B, Papathanassiou D, Crivello F, Etard O, Delcroix N, Mazoyer B, Joliot M. Automated anatomical labeling of activations in SPM using a macroscopic anatomical parcellation of the MNI MRI single-subject brain. Neuroimage. 2002; 15(1):273–289. [PubMed: 11771995]

Vertes RP. Differential projections of the infralimbic and prelimbic cortex in the rat. Synapse. 2004; 51(1):32–58. [PubMed: 14579424]

von Leupoldt A, Sommer T, Kegat S, Baumann HJ, Klose H, Dahme B, Buchel C. The unpleasantness of perceived dyspnea is processed in the anterior insula and amygdala. Am J Respir Crit Care Med. 2008; 177(9):1026–1032. [PubMed: 18263796]

West, JB. Pulmonary Pathophysiology. 4th ed.. Baltimore, MD: Williams and Wilkins; 1992.

Wise RG, Ide K, Poulin MJ, Tracey I. Resting fluctuations in arterial carbon dioxide induce significant low frequency variations in BOLD signal. Neuroimage. 2004; 21(4):1652–1664. [PubMed: 15050588]

Younes, MK.; Remmers, JE. Control of Tidal Volume and Respiratory Frequency. In: Hornbein, TF., editor. Regulation of Breathing: Part I. New York: Marcel Dekker, Inc; 1981. p. 621-671.

Zagon A, Totterdell S, Jones RS. Direct projections from the ventrolateral medulla oblongata to the limbic forebrain: anterograde and retrograde tract-tracing studies in the rat. J Comp Neurol. 1994; 340(4):445–468. [PubMed: 7516349]

Zhang JX, Harper RM, Frysinger RC. Respiratory modulation of neuronal discharge in the central nucleus of the amygdala during sleep and waking states. Exp Neurol. 1986; 91(1):193–207. [PubMed: 3940875]

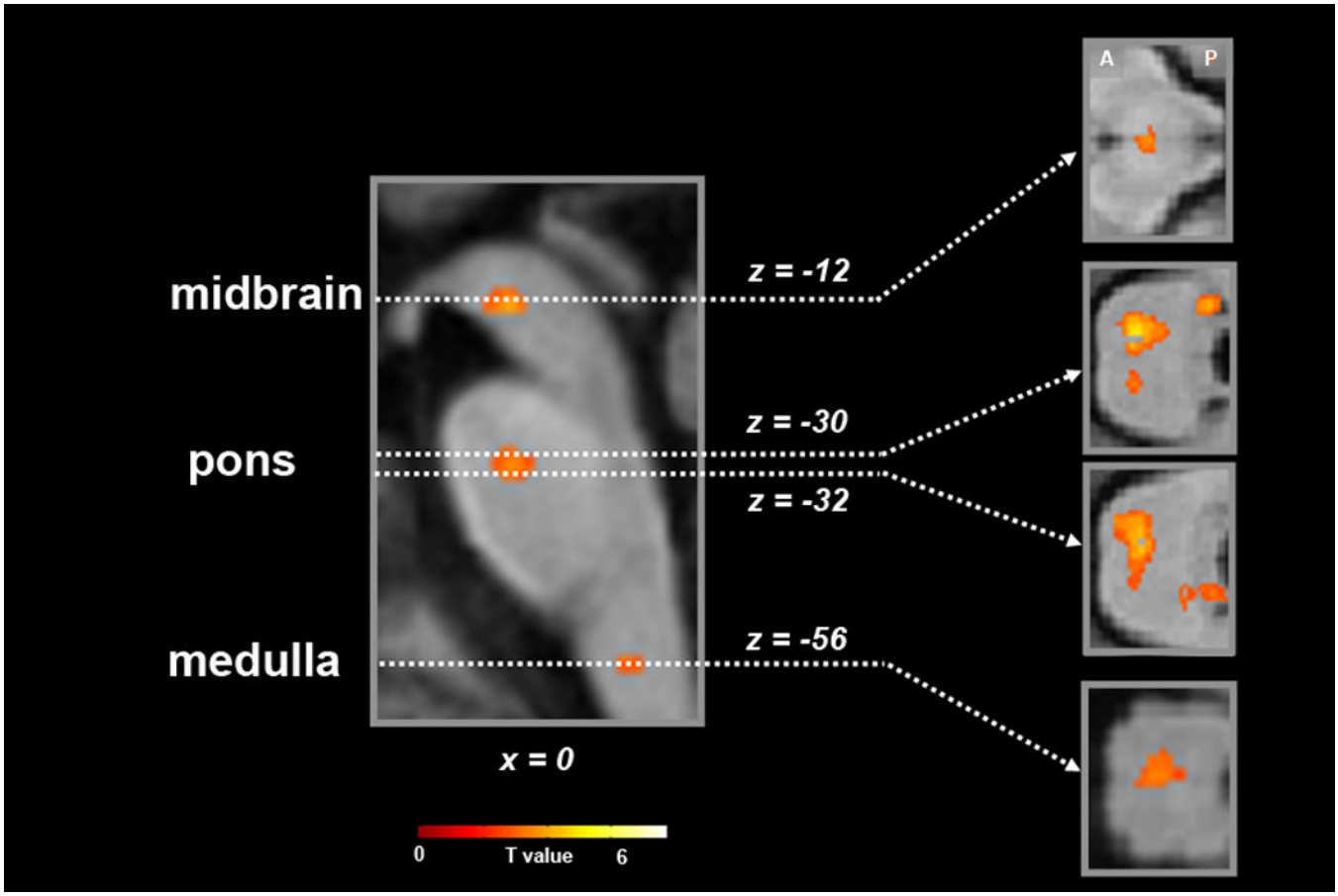

Figure 1.
Statistical maps of neural activity synchronized with the respiratory cycle for the main effects of condition contrast (RNG + BASE), superimposed onto the group mean structural image (n=14). Sagittal slice (x-plane; x=0) is shown on the left and corresponding axial slices (z-planes; z=−12, −30, −32, −56) are shown to the right (MNI coordinate system). Signal intensity is represented by inset color scale (display threshold; $P<5.0 \times 10^{-3}$). Abbreviations: A, anterior; P, posterior.

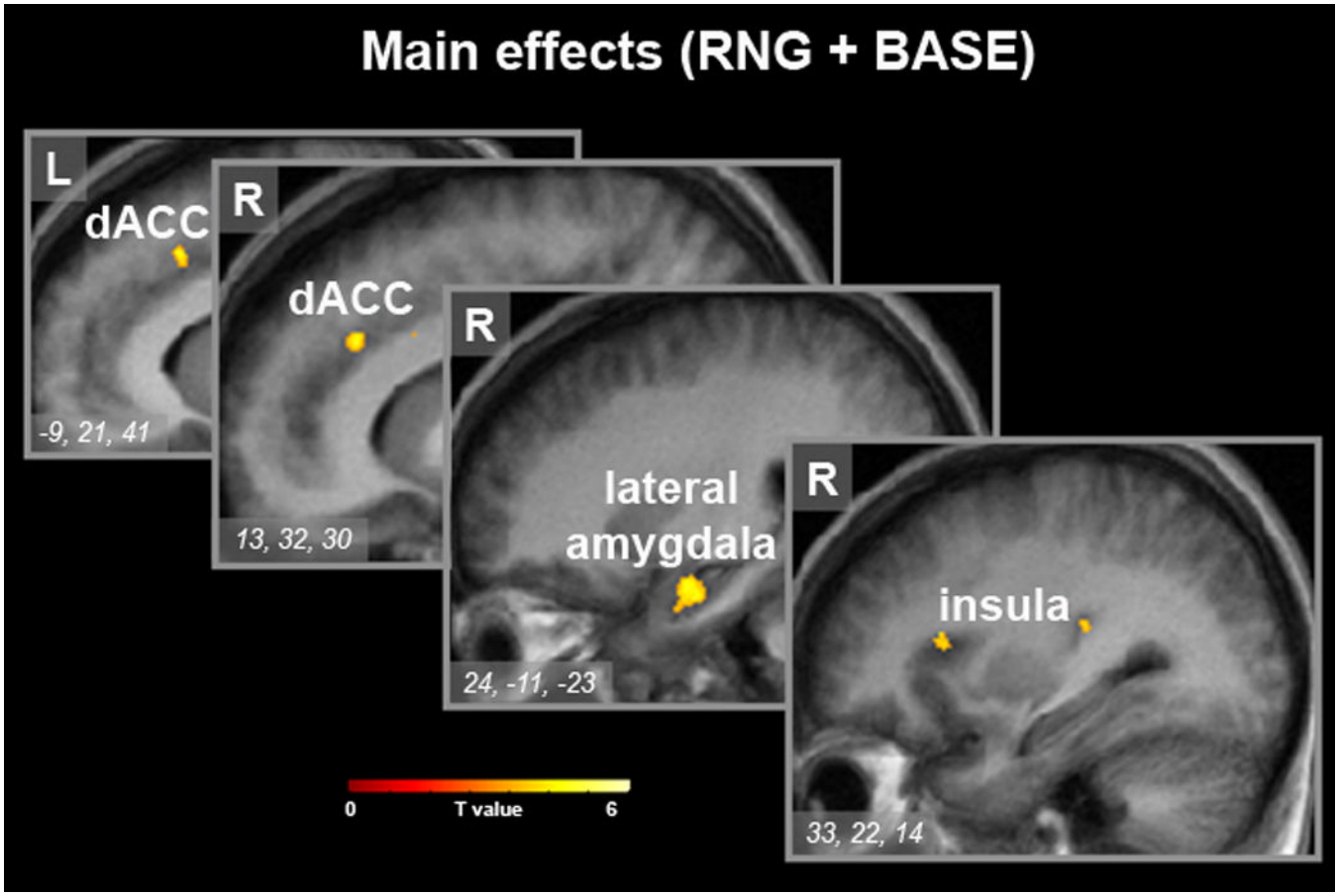

Figure 2.
Statistical maps of neural activity synchronized with the respiratory cycle for the main effects of condition contrast (RNG + BASE), superimposed onto the group mean structural image (n=14). Sequential sagittal slices (x-plane; x=−9, 13, 12, 33) with inset regional maxima are shown (MNI coordinate system). Signal intensity is represented by inset color scale (display threshold; $P<1.6 \times 10^{-4}$, corrected for the limbic search territory). Abbreviations: dACC, dorsal anterior cingulate; L, left; R, right.

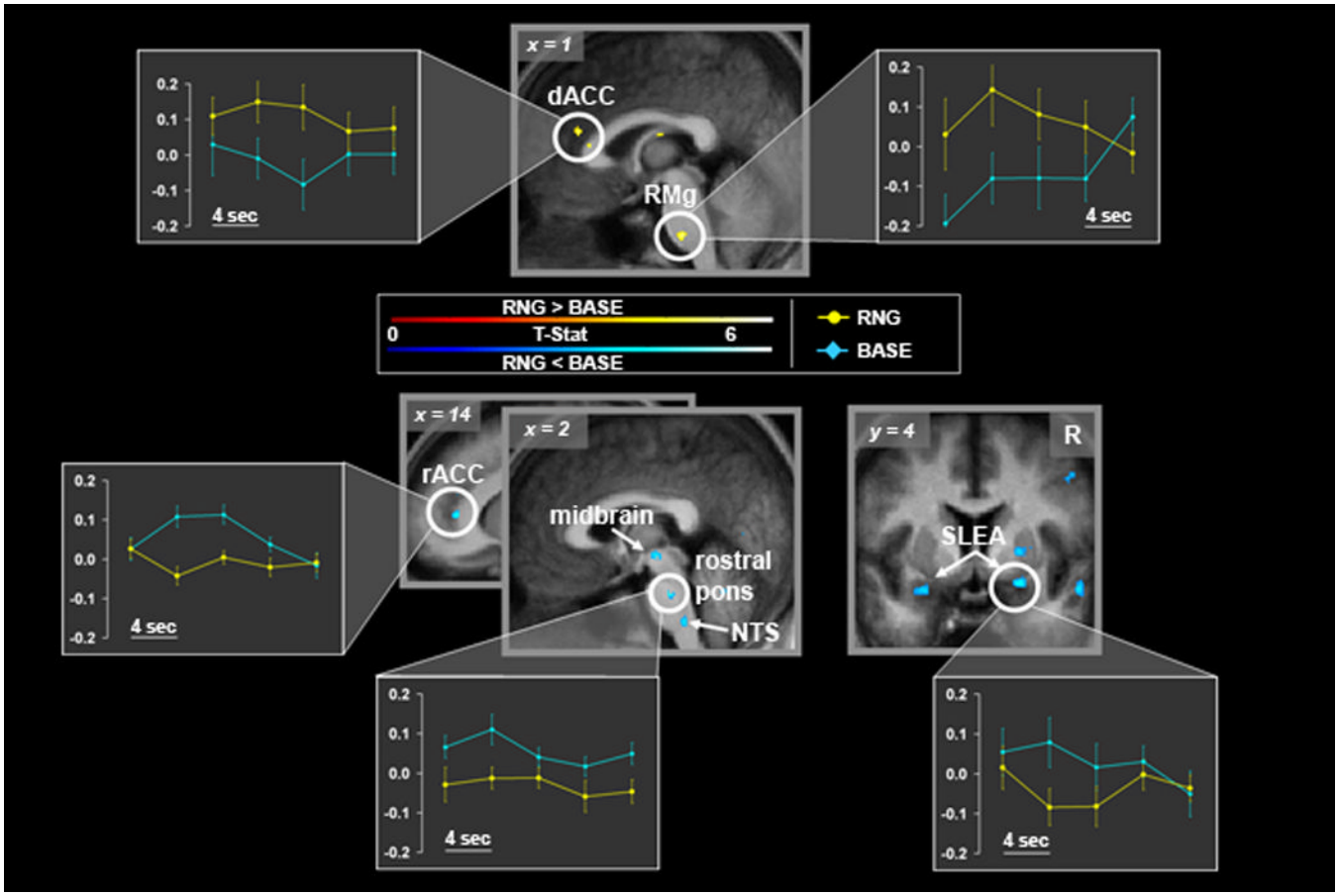

Figure 3.

Statistical maps of differential neural activity synchronized with the respiratory cycle for paired t-tests (RNG > BASE; red-yellow color scale; top, RNG < BASE; blue color scale; bottom), superimposed onto the group mean structural image (n=14). Signal intensity is represented by inset color scales (display threshold; $P<1.6 \times 10^{-4}$, corrected for the limbic search territory). Sagittal and axial slices are shown (MNI coordinate system). Plots depict modeled peri-event (inspiratory onset) BOLD signal time courses for each condition extracted from functional peak clusters (circled) identified by the RNG > BASE and RNG < BASE contrasts (see Experimental Procedures for detail on analytic method). Each point (error bars=standard error of the mean) represents the group averaged regional % BOLD signal change for a given peri- event time bin (4 sec each). The peri-event bins are displayed sequentially from 0–16 sec, to provide a temporal profile of the group mean regional BOLD signal dynamics associated with each breath. The degree of regional neural synchronization with each breath during a given condition can inferred by the degree to which the magnitude and temporal dynamics of the associated BOLD signal time course approximates the canonical BOLD fMRI hemodynamic response function (i.e., 4–8 sec peak, see Results for further details). Abbreviations: dACC, dorsal anterior cingulate; NTS, nucleus tractus solitarius; R, right; rACC, rostral anterior cingulate; RMg, raphe magnus.

Table 1

Results are reported as group mean values ± SD.

Group mean cardio-pulmonary data

	BASE	RNG
P_{CO_2} (mm Hg)	39.40 ± 3.14	39.59 ± 3.29
f_R (breaths/min)	14.57 ± 2.72	15.84 ± 2.64 *
T_I (seconds)	1.77 ± 0.29	1.54 ± 0.23 *
T_E (seconds)	2.58 ± 1.19	2.36 ± 0.61
V_T (liters)	0.41 ± 0.18	0.36 ± 0.15
HR (beats/min)	60.84 ± 9.11	61.12 ± 12.91

Abbreviations: PCO_2, end-tidal partial pressure of CO_2; f_R, breathing frequency; T_I, inspiratory time; T_E, expiratory time; V_T, tidal volume; HR, heart rate.

Asterisk (*) indicates $P < 0.05$ for between condition comparison.

Table 2

Findings for main effects of condition and interaction analyses within *a priori* regions of interest.

Global BOLD signal as regressor of no interest

Contrast	Region	Side	BA	x	y	z	Z score	voxels
RNG + BASE	medulla	L		−1	−37	−57	3.26	12
	rostral pons	L		−5	−22	−31	4.43	110
	midbrain	L		1	−22	−11	3.59	48
	lateral amygdala	R		24	−11	−23	*5.10	570
	dorsal anterior cingulate	L	24	−4	9	23	*5.82	183
		L	32	−9	21	41	*5.40	675
		R	32	9	17	31	*5.13	291
		R	32	13	32	30	4.91	366
		L	24	−5	38	14	4.40	78
	anterior insula	R	45	33	22	14	4.58	146
	posterior insula	L	41	−33	−22	11	*5.86	96
RNG > Base	pons (raphe magnus)	R		2	−25	−43	4.66	184
	dorsal anterior cingulate	L	24	−1	37	18	*5.21	138
		L	24	−1	30	11	5.05	95
RNG < Base	medulla	L		−4	−37	−45	4.73	224
	rostral pons	R		−6	−31	−31	*5.37	163
	midbrain	L		−2	−19	−6	4.35	292
		R		4	−20	−7	4.33	
	rostral anterior cingulate	R	32	14	42	6	4.94	225
	amygdala (SLEA)	L		−26	1	−18	4.81	262
		R		24	4	−14	4.77	92

All reported loci meet regional significance threshold correction for multiple comparisons ($P<0.05$). Asterisk (*) indicates *a priori* loci that also survive whole brain correction (family-wise error, $P<0.05$). Additional *post hoc* loci that survived whole brain correction are reported in Supplemental Table 1. Regional maxima (*x, y, z*) are reported in the MNI coordinate system.

Abbreviations: BA; Brodmann area, BASE; baseline condition, L, left; R, right; RNG, random number generation condition; SLEA, sublenticular extended amygdala.